論文

수지이동 성형공정중 금형충전에 대한 연구 II. 실험적 연구

최미애** · 이미혜*** · 이기준* · 이승종*

Studies on the Mold Filling in the Resin Transfer Molding Process II. Exerimental Studies

Mi Ae Choi**, Mi Hye Lee***, Ki-Jun Lee*, and Seung Jong Lee*

초 록

수지이동성형(RTM)에서 금형충전을 수치모사하기 위해 개발된 컴퓨터 프로그램의 타당성을 실험적으로 검증하였다. 본 연구에서는 투과계수 측정실험, 금형충전 유동가시화 실험과 더불어 동일한 조건하에서 수치모사 실험을 수행하였다. 주어진 공정조건 하에서 금형형태를 다양하게 변화시키면서 충전실험을 행하였다. 섬유보강재가 채워진 투명한 금형 내에서 반응성이 없는 유체를 충전시키며 유동의 선단 진전을 관측하고, 금형형태의 변화에 따른 영향을 고찰하였다. 실험결과와 수치모사 결과를 상호비교해 본 결과, 유동선단의 위치가 수치적으로 예상되었던 것과 잘 일치됨을 볼 수 있었다. 또한, 유동가시화 실험결과로부터 수지이동 성형공정에서 금형충전의 물리적 현상을 해석함으로써 공정의 운전 및 금형설계에 대한 자료를 확보할 수 있었다.

ABSTRACT

To evaluate the validity of the computer program developed to simulate the mold filling in the resin transfer molding (RTM) process, flow visualization experiments of mold filling were conducted. In flow visualization experiments, the measurement of permeability was also carried out. Mold filling experiments were conducted with various types of molds and executed at specified processing conditions. The effects of mold shape variations were studied by observing the movements of the flow font of a non-reactive fluid filling in transparent molds in which fiber reinforcements were preplaced. Experimental observations were compared with corresponding numerical simulation results. Reasonable agreement was obtained between numerically-predicted and experimentally-determined locations of flow front. From the results of visualization experiments, the physical phenomena of the mold filling was able to be interpreted. And also the information for operating the RTM process and designing the mold was obtained.

*서울대학교 화학공학과
**국립기술품질원
***부산지방중소기업청

1. INTRODUCTION

Resin transfer molding(RTM) process is the manufacturing of polymer composite by injecting reactive resins which impregnates the fiber preform and fills the heated mold where it cures to create a composite part. RTM process has the potential of becoming a dominant low cost process for the fabrication of large, integrated, high performance products. The expanded use of RTM composites in high performance products requires efficient structual design methods. Although its potential and benefits have been generally acknowledged and the process is already being used to make parts, there is very little actual information available to guide the designer in the selection of process, equipment and material variables[1-5].

Various studies have been reported in RTM process. A large part of the research effort is the computer simulation of the mold filling process. Also, there are experimental observations on the mold filling flow and studies on various process variables. One of the most important input parameters to simulate the resin transfer molding process is the permeability of fiber mat. Adams et al.[6-8] developed a technique for measuring the in-plane permeability of homogeneous, anisotropic fibrous mat. They also studied the flow of fluids in heterogeneous multilayer constructions and transverse flow mechanism was proposed as being responsible for filling the low permeability layers. Coulter et al.[9-11] undertook the experimental investigation and compared to corresponding numerical results using the boundary-fitted coordinates numerical grid generation. Trevino at al.[12,13] and Young et al.[14] predicted the flow front progression and pressure fields during mold filling by use of finite element/control volume method. Predictions of the model were compared with flow visualization experiments involving permeability variations. Moreover, several researchers have studied the numerical and experimental mold filling in RTM process[15,16].

The first parameter influencing in composite processing is the permeability of fiber reinforcements. For flow visulaization experiment, an accurate value of permeability is required. Several researchers have studied the permeability of fiber mats used in the manufacture of structural composites[7,17-19]. There are still no established permeability measurement methods for fiber mats. Though some measurement techniques have been reported, the measured value of permeability is not accurate since the effect of capillary pressure is not considered. The modified experimental method which is capable of simultaneous measurement of permeability and capillary pressure is proposed in this study. Measured permeability values were used in a numerical simulation to examine the results of mold filling experiment.

We studied on the simulation of mold filling in RTM process in Part I as previously stated. It was focused on the mathmatical numerical method in flow development. In order to validate the previous mold filling program and to interpret the physical phenomena of mold filling, the visualization experiments of mold filling are carried out in this Part II. This paper discusses the methods to determine the values of the permeabilities. Flow visalization experiments are performed using a transparent mold to determine the locaions of the flow front. The experimental results are compared with numerical simulation results.

2. DETERMINATION OF THE PERMEABILITY VALUES

2.1. Radial flow model

Darcy's law relates the fluid flow to the pressure gradient using the fluid viscosity and the permeability of the porous medium.

$$\underline{v} = -\frac{\underline{\underline{K}}}{\mu}\nabla P \quad \cdots\cdots(1)$$

in which $\underline{v}$ is the superficial velocity, μ is the viscosity of the fluid, ∇P is the pressure gradient, and $\underline{K}$ is the permeability tensor of the porous medium. For fiber mats exhibiting circular fronts, the differential equation is obtained as follows ;

$$K_x \frac{\partial^2 P}{\partial x^2} + K_y \frac{\partial^2 P}{\partial y^2} = 0 \quad \cdots\cdots(2)$$

A kinematic condition imposed at the moving front requires that the boundary propagate with the local fluid velocity. For the radial flow, the differential equation obtained from the kinematic condition is ;

$$\frac{dR_f}{dt} = \frac{K\Delta P}{\varepsilon\mu} \frac{1}{R_f \ln(R_f/R_0)} \quad \cdots\cdots(3)$$

where R_f and R_o are the radii at the inlet and liquid front respectively, $K=K_x=K_y$ because of isotropic flow and ΔP is the difference between them. The fiber volume fraction is determined from the properties of the fabric using equation (8) of Part I. Subject to the initial condition ;

$$R_f = R_o \quad \text{at } t=0 \quad \cdots\cdots(4)$$

the solution to equation (3) is ;

$$G(\delta_f) = \frac{\delta_f^2(2\ln\delta_f - 1) + 1}{4} = \Phi \quad \cdots\cdots(5)$$

where δ_f is a dimensionless radial extent and Φ is a dimensionless flow time. These are expressed by following equations ;

$$\delta_f = \frac{R_f}{R_0} \quad \cdots\cdots(6)$$

$$\Phi = \frac{K\Delta P t}{\varepsilon\mu R_0^2} \quad \cdots\cdots(7)$$

Since ΔP is specified experimentally and μ is a known property of the test fluid, discrete $R_f(t)$ data may be plotted in the form of $G(\delta_f)$ versus time as suggested by equation (3). From the slope of the least squares line through the data, m, the isotropic in-plane permeability, K, can be obtained from the following equation ;

$$K = \frac{m\varepsilon\mu R_0^2}{\Delta P} \quad \cdots\cdots(8)$$

In describing impregnation of porous fibrous medium, the contribution of the capillary pressure should be considered, particularly for permeation at low applied pressures. A number of techniques have been focused attention on obtaining more realistic values of permeability. Nevertheless, the validity of techniques has not been extensively established, particularly in the presence of capillary pressure. An improved analytical model for the contribution of capillary pressure to the overall driving force in the impregnation of fibrous medium was presented and direct measurement of the capillary pressure and the unsteady state permeability was suggested.

Considering the effect of capillary pressure, the intrinsic permeability at specified fiber volume fraction could not be directly calculated by the slope of the plot because it was dependent on applied pressure and surface property of fluid. The permeabilities obtained from the slope of the isotropic data plots could not be regarded as intrinsic constants of the fiber mats. Hence, this amounted to replacing K by K_{app} in equation (6) which has the following form ;

$$K_{app} = \frac{m\varepsilon\mu R_0^2}{\Delta P_a} \quad \cdots\cdots(9)$$

The correction for the error introduced by the presence of the capillary pressure was employed in following equation.

$$K_{intr} = \frac{m\varepsilon\mu R_0^2}{\Delta P_a + \Delta P_c} \quad \cdots\cdots(10)$$

As easily shown by equation (10), in the presence of high applied pressure, the relative contribution of the capillary pressure was reduced. Looking into the above equation, the intrinsic permeability could be calculated from the slope of a curve, which was plotted the product of apparent permeability and applied pressure as a function of applied pressure under specified fiber volume fraction.

2.2. Permeability Measurement

The experiments to measure the isotropic permeability of commercial fiber mats were undertaken and the experimental apparatus was manufactured as illustrated in Fig. 1. Two 30×30cm square plates formed the upper and lower boundaries of a radial flow region. The upper transparent acrylate plate permitted visual observation of the in-plane flow process. A 1 cm diameter inlet hole was centered in the lower plate, and spacers of constant thickness were used to maintain a uniform thickness in the layered fiber mats between the mold plates. Compressed nitrogen gas was used to push the liquid through the fiber mats placed between two mold plates. The radial position and the shape of the advancing front were monitored as a function of time. Discrete time data were typically taken in at radial intervals of about 0.5 cm. At least three specimens are used to characterize fiber mats and the experimental results are averaged.

Silicone oil was used as the experimental fluid. The viscosity of the fluid at room temperature was measured using a cone and plate geometry on a Rheometrics Mass Spectrometer. The silicone oil exhibited a behavior of Newtonian fluid. The fiber material used in this study was Kevlar mat of 3/1 twill weave type supplied by DuPont Co. The surface density of the fiber mat and the fiber density were measured as 0.0173g/cm^2 and 1.44g/cm^3, respectively.

2.3. Permeability Calculation

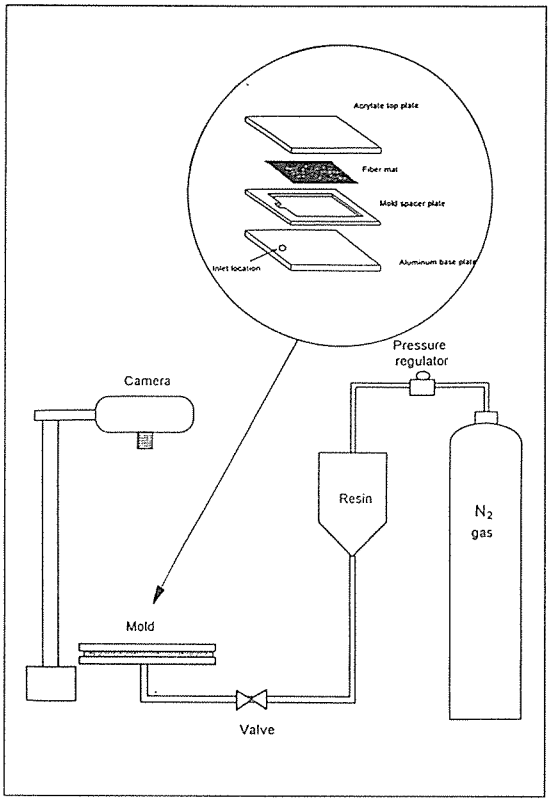

Fig. 1. Schematic diagram of the experimental apparatus used in this study

Experimental data for the Kevlar fiber mat were shown in Fig. 2, in which $G(_f)$ versus time due to variation of applied pressure was plotted. As clearly shown in this figure, in all three cases the data correlated well with least squares lines. This linear relationship was observed for the fiber mats with a constant fiber volume fraction of 0.3844. The permeability obtained from the slopes of the isotropic data plots was property constants of the fiber mats.

We experimentally investigated the effects of applied pressure on apparent permeability. The apparent permeability was measured as the applied pressure varied from 0.5×10^5 to $1.55\times10^5 P_a$. The fluid with viscosity of 2.6 Pa · s was selected. As shown in Fig. 3, the apparent permeability was decreased with the increase of the

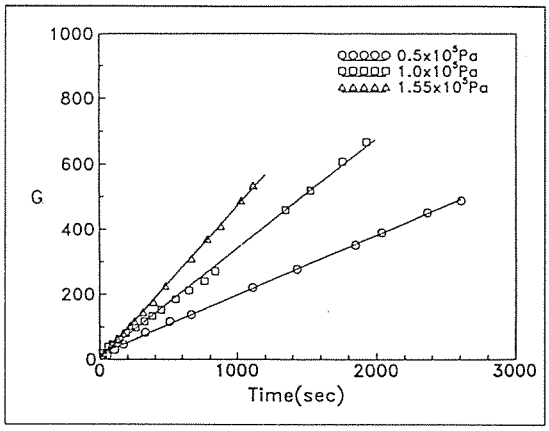

Fig. 2. Variation of function G vs. time for Kevlar fiber mats at V_f=0.3844 under the various pressures

applied pressure. This was explained by that as more high pressure was applied, the capillary effects became negligible. In Fig. 4, as expected, a linear relationship was observed. This linearity confirmed the validity of the analysis suggested in this study. From this figure, the permeability determined as the slope of the plot was $1.0976\times 10^{10}m^2$ at the fiber volume

fraction of 0.3844. The capillary pressure was also calculated as the horizontal axis intercept value and the value was 1.85×10^4P_a.

It was argued that the capillary pressure could be comparable to the applied pressure as the liquid advanced through dry fiber mats. But as the

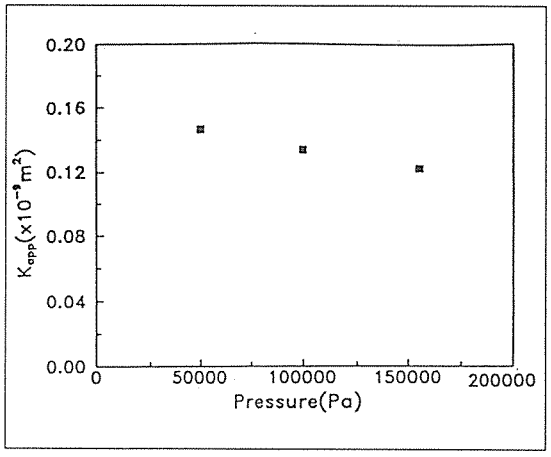

Fig. 3. The pressure dependence of the apparent permeability

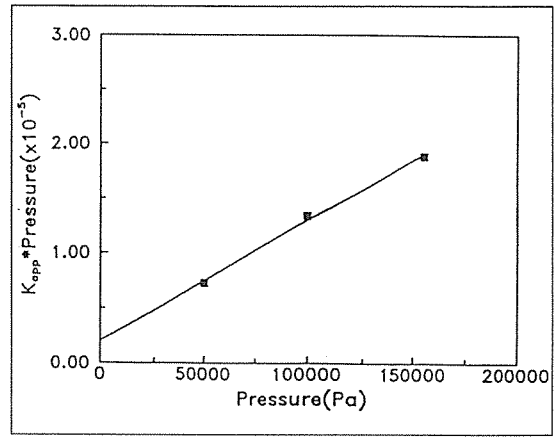

Fig. 4. The plot of $K_{app} * P$ vs. P to determine the capillary pressure in the filling of silicone oil through Kevlar fiber mats

capillary pressure term in equation (10) was small, it might be neglected and approximate values of apparent permeability could be obtained directly from Fig. 2. In conclusion, permeability measurement techniques developed in this study could provide more realistic value of permeability.

3. FLOW VISUALIZATION EXPERIMENTS

A number of simple experiments were conducted to achieve a better understanding of the physics of resin transfer molding process and to verify the results of the numerical simulation. The experimental apparatus was used the same as that of permeability measurement illustrated in Fig. 1. A flat plate mold was used consisting of two plates held apart by a spacer plate. The top plate was made of acrylate in order to monitor the flow progression on camera. The gap height could be varied by inserting the mold spacer with different thickness. The fiber mats were surrounded by the mold spacer. After positioning the fiber mats and closing the mold, the fluid was injected at the edge from a pressure tank. The driving pressure was set by

Table 1. Materials properties and processing conditions used in the numerical simulations and experiments of mold filling.

Materials Properties	fluid	silicone oil
	viscosity	2.6 Pa · s
	fiber mat	Kevlar, 3/1 twill weave
	permeability	$1.21741 \times 10^{-10} m^2$
Processing Conditions	mold thickness	1.25mm
	inlet gate width	2cm
	fiber volume fraction	0.3844
	inlet pressure	1.55×10^5Pa

pressurizing the space silicone oil with compressed nitrogen. The pressure at the inlet gate was held constant using a pressure gauge to adjust the tank pressure. Photographs were taken during mold filling from the top to determine the flow front position at each time step. The material properties and processing conditions used in these experiments were listed in Table 1.

4. RESULTS AND DISCUSSION

In order to validate the predicted mold filling results obtained from the numerical simulation, simple experiments were carried out.

For rectangular mold, the experimental and numerical flow fronts were represented at specified filling time step. As seen in Fig. 5, the experimental flow fronts agreed reasonably well with the numerical predictions. The shape of the flow front was initially circular around the injection port as expected from numerical simulation. It could be seen from the numerical results that as the flow progressed, the resin front gradually revealed the shape of straight line. However, the experimentally observed resin fronts did not show straight line and the observed movement of contact point at mold wall lagged the numerical movement throughout filling. This deviation might be related to the installation of the mats inside the mold. The fiber mats were cut manually and it was difficult to obtain a consistently

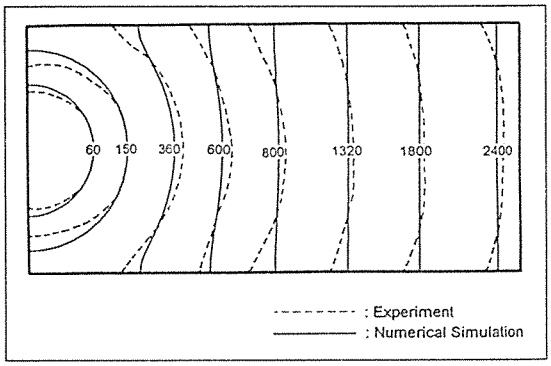

Fig. 5. Experimental and numerical flow front locations in the filling of the rectangular mold cavity ($t_{fill,exp}$=2640s, $t_{fill,num}$=2608s)

straight cutting. When the fiber mats were compressed inside the mold, along the edges the fiber mats could get squeezed or exceed slightly the clearance of the mold. Thus, this phenomenon decreased the local permeability along the edges as observed in experiment. The change in permeability due to these causes might vary for each experiment and it was difficult to evaluate the effects quantitatively. The fill time in experiment was observed as 2640s and in simulation it was calculated as 2608s. The quantitative agreement between the sets of data was reasonable.

Fig. 6 showed the experimental and numerical results of flow front locations at different filling time step for the square mold. The fill time was observed experimentally 3780s. This fill time was less than the predicted fill time of 4051s. This lack of quantitative correlation could be attributable to several factors including the explanation mentioned above. From the figure it could be seen that the predicted and experimental flow front corresponded relatively well. However, the experimentally observed resin fronts showed a dissymmetry between the top and bottom wall. As the injection port was located on a horizontal middle line, the numerical results displayed a symmetrical progression of the resin front. At bottom wall the experimental flow front moved faster along the mold wall. This effect was also observed fre-

quently during the experiments. Some deviation seen in Fig. 6 was probably due to the flow channeling between the reinforcements and the edge of the mold. The fiber mats did not fit the mold surface exactly, which resulted in lowering of the fiber volume fraction near the mold wall. This often occurred even if the fiber mats were completely against the wall which was the case here. Looking at both Fig. 5 and Fig. 6, it was noted that even a slight shift in the position of the fiber mats had a significant effect on the flow near the walls. This meant that the permeability near the wall was very sensitive to the positioning of the fiber mats in the mold. Thus there was practical limitations to model accurately for RTM process.

Also, this lack of close correlation between in experimental and numerical flow front could be explained as numerical error. The computational complications might arise from the determination of the boundary conditions that applied at the contact point of the free surface with mold walls.

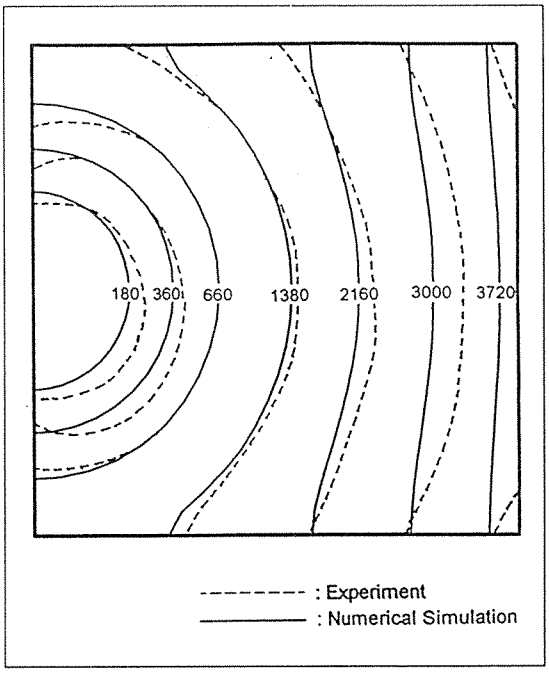

Fig. 6. Experimental and numerical flow front locations in the filling of the square mold cavity ($t_{fill,exp}$=3780s, $t_{fill,num}$=4051s)

Throughout the numerical simulation corresponding in these cases, full slip movement of the free surface at mold wall contact points was applied. Two notable features appeared in the experiment results. First, the resin established preferred flow paths along the edges where the fiber volume fraction was lower. The existence of fiber termination as in this case could lead to the observance of a slip like phenomenon in the near wall regions. Second, the flow fronts were delayed in small localized regions of lower permeability by compacted fiber mats. The resin front movement at contact point of mold wall showed that a no slip type flow condition existed along the mold wall. In order to model the resin flow more accurately, it could be suggested that the modification of boundary condition at contact point should be necessary. And the best type boundary condition might be one of partial slip, with degree of slip depending on exact mold and preform configuration.

Fig. 7 showed the experimental and numerical results for two opposite flow directions for the mold with linear variations along its length. For diverged mold the fill time of 3240s was experimentally obtained and 3068s was numerically calculated. For converged mold, the experimental value was 2940s and the numerical value was 2802s. Although there were some deviations for the same mold configuration, the experimental results corresponded qualitatively well with the numerical results. Here, we proved the conformity of numerical results by the experimentation. Again it could be announced that as far as the fill time was concerned, the converged mold was favorable in comparison with the diverged mold.

Fig. 8 showed the comparison of the flow fronts for the mold with the round insert. In experiment the fill time was observed as 2660s and in numerical simulation it was calculated as 2789s. Agreement between predicted and experimental front locations was good until the front reached the insert. But there were some discrepancies in the

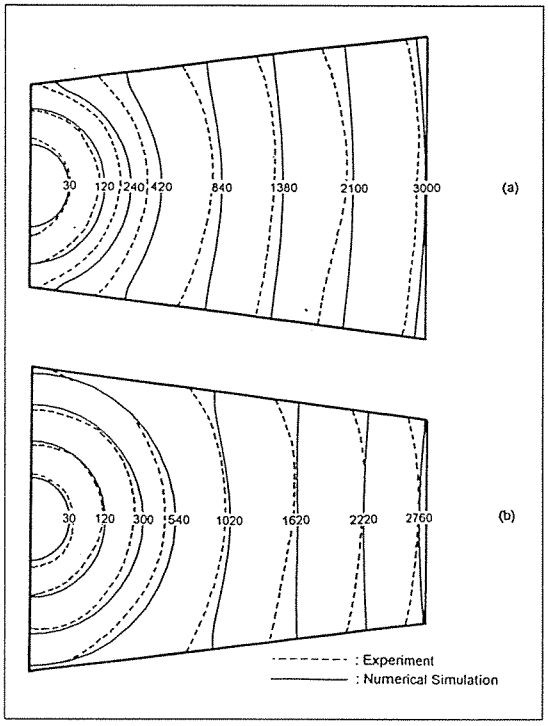

Fig. 7. Experimental and numerical flow front locations in the filling of the width-tapered mold cavity ; (a)width-diverged ($t_{fill,exp}$=3240s, $t_{fill,num}$=3068s), (b)width-converged ($t_{fill,exp}$=2940s, $t_{fill,num}$=2802s)

shape of the flow front in the region after the insert, where the flow tended to move faster in experiment. Two possible explanations of this effect were given. The first was explained by the fact that perhaps the fiber volume fraction in the rear of insert was actually less than that given initially. Since the mold tended to deform when the mold was clamped together, it was likely that the mold thickness was increased by inserting the round part. Therefore the fiber volume fraction changed by some variation in mold thickness, causing the increased permeability. Another was illustrated in numerical side that the boundary condition posed at insert might not be appropriate since it was difficult to fit exactly the fiber mats on the surface of the inserted object.

It is clear from our results that although we were able to predict flow front movement for relatively complex geometries under variable processing conditions, we still need further understanding of flow phenomena connected with interactions between the fluid and the fiber mats. Furthermore, it is necessary to predict how the permeability of the fiber mats is influenced by non consistencies near the mold walls and to determine the appropriate boundary condition in order to match exactly the conditions of experimentation.

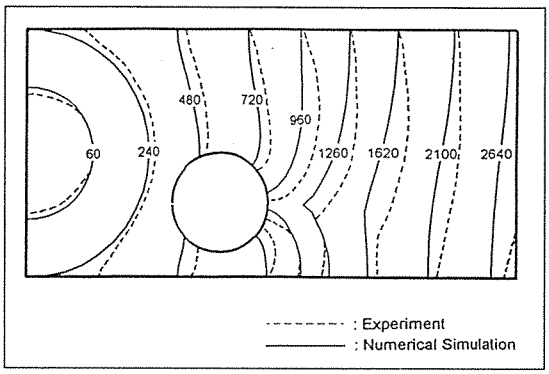

Fig. 8. Experimental and numerical flow front locations in the filling of the mold cavity with a circular insert ($t_{fill,exp}$= 2660s, $t_{fill,num}$=2789s)

5. CONCLUSIONS

An experimental and numerical analysis of mold filling in the resin transfer molding process was carried out to test the computer program developed in previous paper Part Ⅰ.

In permeability measurement techniques, a simplified analytical model for evaluating the contribution of capilliary pressure during the impregnation of fibrous media was proposed. The limited experimental results indicated that the existence of the capillary effect could be often significant.

Visualization experiments of mold filling were carried out over five types of mold geometry. From flow visualization experiments, important information of the filling process can be obtained, which is valuable in the design of tooling and processes. Above of all, the modification of

boundary condition at the contact point along the wall should be necessary. Consequently, it was found that the observed experimental behavior agreed well with the numerically predicted results.

NOMENCLATURE

$\underline{K}$	permeability tensor
K_{app}	permeability at applied pressure
K_{intr}	intrinsic permeability
P	pressure
P_a	applied pressure
P_c	capillary pressure
R_o	radius at the innlet
R_f	radius of liquid front
t	time
$\underline{v}$	superficial velocity
x, y	global coordinates

Greek letters

δ_f	dimensionless radial extent
ε	porosity
v	viscosity
Φ	dimensionless flow time

REFERENCES

1. Owen, M.J., Rudd, C.D. and Middleton, V., "Effects of Process Variables on Cycle Time During Resin Transfer Molding for High Volume Manufacture," Materials Science and Technology, Vol.6, 1990, p. 656.

2. Karbhari, V.M., Slotte, S.G., Steenkamer, D.A. and Wilkins, D.J., "Effects of Materials, Process, and Equipment Variables on the Performance of Resin Transfer Molded Parts," Composites Manufacturing, Vol.3, No.3, 1992, p. 143.

3. Hayward, J.S. and Harris, B., "Processing Factors Affecting the Quality of Resin Transfer Moulded Composites," Plastics and Rubber Processing and Applications, Vol.11, No.4, 1989, p. 191.

4. Hayward, J.S. and Harris, B., "Effect of Process Variables on the Quality of RTM Mouldings," SAMPE Journal, Vol.26, No.3, 1990, p. 39.

5. Stover, D., "Resin Transfer Molding for Advanced Composites," Advanced Composites, March/April, 1990, p. 60.

6. Adams, K.L., Miller, B. and Rebenfeld, L., "Forced In-Plane Flow of an Epoxy Resin in Fibrous Networks," Polym. Eng. Sci., Vol.26, No.20, 1986, p. 1434.

7. Adams, K.L. and Rebenfeld, L., "In-Plane of Fluids in Fabrics: Structure/Flow Characterization," Textile Research Journal, Vol.57, 1987, p. 647.

8. Adams, K.L. and Rebenfeld, L., "Permeability Characterization of Multilayer Fiber Reinforcements. Part I: Experimental Observation," Polymer Composites, Vol.12, No.3, 1991, p. 179.

9. Coulter, J.P., Smith, B.F. and Guceri, S.I., "Experimental and Numerical Analysis of Resin Impregnation During the Manufacturing of Composite Materials," Proc. 2nd Tech. Conf., ASC, 1987, p. 209.

10. Coulter, J.P. and Guceri, S.I., "Resin Impregnation During the Manufacturing of Composite Materials Suject to Prescribed Injection Rate," J. of Reinforced Plastics and Composites, Vol.7, 1988, p. 200.

11. Coulter, J.P. and Guceri, S.I., "Resin Impregnation During Composites Manufacturing: Theory and Experimentation," Composites Sci. and Tech., Vol.35, 1989, p. 317.

12. Trevino, L., Rupel, L., Young, W.B., Liou, M.J. and Lee, L.J., "Analysis of Resin Injection Molding in Molds with Preplaced Fiber Mats. 1. Permeability and Compressibility Measurements," Polymer Composites, Vol.12, No.1, 1991, p. 20.

13. Trevino, L., Rupel, L., Young, W.B., Liou, M.J. and Lee, L.J., "Analysis of Resin Injection Molding in Molds with Preplaced Fiber Mats. 2. Numerical Simulation and Experiments of Mold Filling," Polymer Composites, Vol.12, No.1,

1991, p. 30.

14. Young, W.B., Han, K., Fong, L.H., Lee, L.J. and Liou, M.J., "Flow Simulation in Molds with Preplaced Fiber Mats," Polymer Composites, Vol.12, No.6, 1991, p. 391.

15. Um, M.K. and Lee, W.I., "A Study on the Mold Filling Process in Resin Transfer Molding," Polym. Eng. Sci., Vol.31, No.11, 1991, p. 765.

16. Chan, A.W. and Hwang, S.T., "Modeling of the Impregnation Process During Resin Transfer Molding," Polym. Eng. Sci., Vol.31, No.15, 1991, p. 1149.

17. Skartisis, L., Kardos, J.L. and Khomami, B., "Resin Flow Through Fiber Beds During Composite Manufacturing Processes. Part I: Review of Newtonian Flow Through Fiber Beds," Polym. Eng. Sci., Vol.32, No.4, 1992, p. 1.

18. Wu, C.H., Wang, T.J. and Lee, L.J., "In-Plane Permeability Measurement and Analysis in Liquid Composite Molding," Polymer Composites, Vol.15, No.4, 1994, p. 278.

19. Wu, C.H., Wang, T.J. and Lee, L.J., "Trans-Plane Fluid Permeability Measurement and Its Applications in Liquid Composite Molding," Polymer Composites, Vol.15, No.4, 1994, p. 289.